THE INFLUENCE OF THIN BONDING LAYERS ON THE LEAKY WAVES AT LIQUID-SOLID INTERFACES

by

A. H. Nayfeh
Systems Research Laboratories, Dayton, Ohio 45440

D. E. Chimenti, Laszlo Adler, and R. L. Crane
AFWAL Materials Laboratory, Wright-Patterson AFB, Ohio 45433

ABSTRACT

This paper presents theoretical and experimental results on the problem of bounded acoustic beam reflection at the Rayleigh angle from a fluid-solid interface which is loaded by a thin solid layer. The theoretical development exploits the framework of existing theory to yield a simple, analytic model which is reasonably accurate for thin layers. It is shown that the influence of the layer is contained entirely in the dispersive Rayleigh wavespeed and the thickness-dependent displacement parameter Δ_s. Measurements of the reflected acoustic field amplitude have been performed on several samples of stainless steel loaded with a thin copper layer. We have found reasonably good agreement between the theoretical model calculations and experimental measurements for ratios of the layer thickness to the Rayleigh wavelength as large as 0.3. Beyond this value, some disparity is observed, particularly in the calculation of the thickness-dependent Rayleigh wavespeed.

INTRODUCTION

The energy redistribution that occurs when a bounded acoustic beam is reflected from a fluid-solid interface has been the subject of many analytical and experimental investigations. Following the discovery of analogous effects in optics by Goos and Hänchen [1], Schoch predicted [2]--and later experimentally verified [3]--the beam-displacement effect for an acoustic beam incident on a liquid-solid interface. According to Schoch's predictions, the beam is nonspecularly reflected since it is laterally displaced while retaining, more or less, its original profile. In contrast to these predictions, many experiments [4-7] have revealed that the reflected beam may also suffer severe distortion if it is incident at, or near, the Rayleigh angle. Physically what occurs is the resonant transfer of acoustic energy from a longitudinal wave in the liquid to a pseudo-Rayleigh wave propagating along the liquid-solid interface. As it propagates, the Rayleigh wave re-radiates into the liquid at the Rayleigh angle because of this resonant coupling. The result is a redistribution of the reflected field intensity such that a sizable fraction of the acoustic energy seems linearly displaced along the interface. This energy redistribution includes, in addition to the lateral displacement, a null region and a trailing field which becomes weaker as it extends along the interface away from the incident beam.

Bertoni and Tamir [8] have examined the reflection coefficient for angles close to the Rayleigh angle and constructed a model which explains these distortion phenomena. Specifically, they pointed out that the suitably simplified reflection coefficient has a singularity which leads to solutions corresponding to radiating (leaky) Rayleigh waves. According to their analysis, the distortion is the result of interference between the geometrically reflected field and the field of a leaky Rayleigh wave created by the incident beam at the Rayleigh angle. Breazeale, Adler, and Scott [9] experimentally verified the Bertoni and Tamir model, while Pits, Plona, and Mayer [10] have recently presented theoretical results for the case of a finite beam incident on a solid plate in a liquid. Their results show that distortion of the reflected beam at the Lamb angle can also occur.

This paper investigates theoretically and experimentally, the influence of a thin layer bonded to a solid upon the shift and distortion of the reflected beam. This problem differs from the no-layer case in that the reflection coefficient is not readily available in closed form, and therefore must be derived. The results of this analysis reveal new phenomena that occur in the presence of the layer. Both the Rayleigh wavespeed and the parameter associated with the energy redistribution are frequency dependent in the layer case. These two new effects, in turn, influence the lateral displacement and distortion of the reflected beam.

THEORY

Formulation of the Problem

Consider a thin elastic layer of thickness 2h in welded contact with a solid elastic half-space of different material. Overlying this structure is a fluid (water) half-space as shown in Fig. 1. A coordinate system is chosen with the origin located at the center of the layer and with the positive z-axis pointing downward into the semi-infinite solid. The layer extends from $-h \le z \le h$, with the solid half-space extending from $z = +h$ to ∞ and the fluid extending from $z = -h$ to $-\infty$. In our subsequent analysis we shall identify the field variables and properties of the layer, fluid, and solid substrate with the subscripts o, f, and s, respectively. The fluid medium is subjected to a time-harmonic, bounded acoustic beam incident onto the fluid-solid interface at an angle θ_i with respect to the surface normal. To reduce the analysis to two dimensions, we assume that no acoustic wave, incident or reflected, has a y-dependence. Alternatively, all particle motion is confined to the x-z plane.

To study the behavior of the reflected beam, one must solve the appropriate field equations in each of the three media (liquid, layer, and substrate), incorporating the appropriate continuity conditions. Formal solutions are obtained by introducing the potential functions ϕ and ψ for each of the media. These functions are related to the particle velocities and stresses by

$$\dot{u} = \frac{\partial \phi}{\partial x} - \frac{\partial \psi}{\partial z} \tag{1}$$

$$\dot{w} = \frac{\partial \phi}{\partial z} + \frac{\partial \psi}{\partial x} \tag{2}$$

$$\sigma_z = (\lambda+2\mu) \frac{\partial^2 \phi}{\partial z^2} + \lambda \frac{\partial^2 \phi}{\partial x^2} + 2\mu \frac{\partial^2 \psi}{\partial x \partial z} \tag{3}$$

$$\sigma_{xz} = \mu \left[2 \frac{\partial^2 \phi}{\partial x \partial z} + \frac{\partial^2 \psi}{\partial x^2} - \frac{\partial^2 \psi}{\partial z^2} \right] . \tag{4}$$

where u and w are displacements parallel to the x and z axes, respectively. The terms λ and μ are the familiar Lame' constants and σ_z and σ_{xz} are the normal and shear stresses, respectively. The dot above a variable, such as u, denotes differentiation with respect to time. Since the fluid cannot support a shear wave, the shear potential ψ is identically zero in this medium. In the two solid media ψ has only a single nonvanishing component because particle motion is restricted to the plane of incidence.

The wave potentials ϕ and ψ satisfy separate wave equations for linear, isotropic media, namely

$$\frac{\partial^2 \phi}{\partial x^2} + \frac{\partial^2 \phi}{\partial z^2} = \frac{1}{c_1^2} \frac{\partial^2 \phi}{\partial t^2} , \tag{5a}$$

$$\frac{\partial^2 \psi}{\partial x^2} + \frac{\partial^2 \psi}{\partial z^2} = \frac{1}{c_2^2} \frac{\partial^2 \psi}{\partial t^2} . \tag{5b}$$

The longitudinal and shear wavespeeds for each medium are given respectively by

$$c_1 = \left(\frac{\lambda+2\mu}{\rho} \right)^{\frac{1}{2}} , \quad c_2 = \left(\frac{\mu}{\rho} \right)^{\frac{1}{2}} , \tag{6}$$

where ρ is the density of the medium. The subscripts 1 and 2 denote longitudinal and shear properties, respectively. Solutions of Eqs. (1) - (6) must also satisfy the continuity conditions at the interfaces; in our notation these are

$$u_s = u_o, \; w_s = w_o, \; \sigma_{zs} = \sigma_{zo},$$

$$\sigma_{xzs} = \sigma_{xzo}, \text{ at } z = h \tag{7}$$

$$w_o = w_f, \; \sigma_{zo} = \sigma_{zf}, \; \sigma_{xzo} = 0, \text{ at } z = -h . \tag{8}$$

Reduced Model

In principle, solutions to Eqs. (1) - (5), subject to the continuity conditions of Eqs. (7) and (8), could be formally obtained, but the results would be quite complicated algebraically. Moreover, an attempt to obtain an exact solution could obscure important features of the problem. Therefore, since our principal interest in this problem

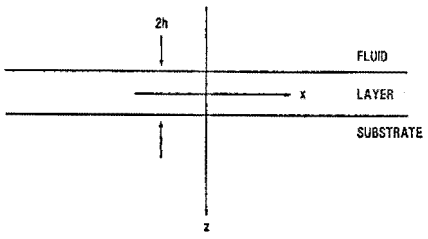

Figure 1 - Coordinate geometry

centers on the case of a thin layer, we include the effect of the layer as a nonzero, homogeneous term in the boundary conditions. To this end we rewrite Eqs. (1) - (5) for the layer in terms of displacements and stresses, average these equations across the layer thickness and satisfy the boundary conditions (7) and (8). We neglect the variations in the displacements u_o and w_o to obtain the substitute fluid interface conditions as a first order approximation in h

$$2h \left[(\lambda_o+2\mu_o) \frac{\partial^2 u_o}{\partial x^2} - \rho_o \ddot{u}_o \right] = -\sigma_{xzs}(0) \tag{9}$$

$$2h \left[\mu_o \frac{\partial^2 w_o}{\partial x^2} - \rho_o \ddot{w}_o \right] = \sigma_{zf}(-0) - \sigma_{zs}(0) . \tag{10}$$

Equations (9) and (10) are significant since they are the only relations that contain the effect of the layer via the modified longitudinal and shear stress boundary conditions. In the absence of the layer (h = 0) they reduce to $\sigma_{zs}(0) = \sigma_{zf}(0)$, $\sigma_{xzf}(0) = 0$, which are the classical liquid-solid stress continuity relations.

Reflection Coefficient and Leaky Wave Dispersion

To determine the reflection coefficient for plane harmonic waves incident from a fluid onto a solid surface, we begin by writing the Fourier transforms of the wave potentials with respect to the x-coordinate and assume exponential solutions in the z-coordinate. These steps lead to formal solutions given by

$$\hat{\phi}(\xi) = \Phi e^{i\zeta_1 z} , \quad \hat{\psi}(\xi) = \Psi e^{i\zeta_2 z} \tag{11a,b}$$

and

$$\hat{\phi}_f(\xi) = \Phi_f e^{i\zeta_f z} + \Phi_f' e^{-i\zeta_f z} , \tag{11c}$$

where the caret indicates a transform, and the prime designates a reflected field. The circular frequency is ω, and the complex amplitudes Φ, Ψ,

Φ_f, and Φ'_f are constants to be determined from the boundary conditions. The wavevector components are given by

$$\zeta_{1,2} = (k^2_{1,2} - \xi^2)^{\frac{1}{2}} , \quad \zeta_f = (k^2_f - \xi^2)^{\frac{1}{2}} \qquad (12)$$

where $\xi \equiv k_f \sin\theta$ with the angle θ measured from the surface normal. The longitudinal and shear wavenumbers are $k_{1,2} = \omega/c_{1,2}$. In the fluid we shorten this notation to $k_f = \omega/c_f$, since there can be no ambiguity. From Eq. (11c) the reflection coefficient, R, is given by

$$R = \Phi'_f/\Phi_f . \qquad (13)$$

Inserting the Fourier transformed stresses and displacements into the continuity conditions, Eqs. (7) and (8), yields a system of linear equations that relate the wave potential amplitudes. Using these relations the value of R becomes

$$R = \frac{\zeta_f (a_1 b_2 + a_2 b_1) + \rho_f \omega^2 (\xi a_2 - \zeta_{1s} b_2)}{\zeta_f (a_1 b_2 + a_2 b_1) - \rho_f \omega^2 (\xi a_2 - \zeta_{1s} b_2)} \qquad (14)$$

where

$$a_1 = \mu_s (2\xi^2 - k^2_{2s}) - 2ih\mu_o \zeta_{1s} \zeta^2_{2o} \qquad (15a)$$

$$b_1 = 2i\xi [i\mu_s \zeta_{2s} - h\mu_o \zeta^2_{2o}] \qquad (15b)$$

$$a_2 = 2i\xi [i\mu_s \zeta_{1s} - h(\lambda_o + 2\mu_o)\zeta^2_{1o}] \qquad (15c)$$

$$b_2 = \mu_s (2\xi^2 - k^2_{2s}) - 2ih\zeta_{2s}(\lambda_o + 2\mu_o)\zeta^2_{1o} . \qquad (15d)$$

In the absence of the layer (h = 0) Eq. (14) correctly predicts the reflection coefficient of a liquid-solid interface (see [13] for example). Now we consider the dispersion of the propagating surface waves at the liquid-solid interface. This dispersion is produced by the layer and, therefore, vanishes in its absence.

The expression Eq. (14) for the reflection coefficient contains, as a by-product, the characteristic equation for the propagation of a modified ("leaky") Rayleigh surface wave which propagates along the interface between the fluid and the thin layer bonded to the solid. The vanishing of the denominator in Eq. (14),

$$\zeta_f (a_1 b_2 + a_2 b_1) - \rho_f \omega^2 (\xi a_2 - \zeta_{1s} b_2) = 0 \qquad (16)$$

is the characteristic equation for such waves. If Eq. (15) is substituted into Eq. (16), then for a real frequency ω, Eq. (16) will admit complex solutions of the form

$$\xi = k_r + i\alpha . \qquad (17)$$

From Eq. (17) the phase velocity of the Rayleigh wave is given as $c_r = \omega/k_r$, and α is the attenuation coefficient. Note that α vanishes in the absence of the fluid, and hence no attenuation (leaking of energy in the fluid) occurs. In the presence of a fluid these surface waves are called "leaky waves." It will later be shown, as has been done by others [10], that c_r is hardly affected by the presence of the fluid, and therefore, α is very small. However, as shown by Bertoni and Tamir [8], α is important because it is related to the lateral displacement of the reflected beam. Examination of Eq. (16) indicates that in the layer case, the medium is dispersive, and both c_r and α depend on the frequency in a rather complicated fashion. Notice also that Eq. (16) contains the classical characteristic equation for a surface wave, which is obtained by setting h = 0 and ρ_f = 0. Graphical results of c_r as a function of frequency are presented and compared to measurements in Section IV.

Field of the Reflected Beam

In this section we discuss the reflection of a finite-width beam having a Gaussian profile which is incident on the liquid-solid interface at an angle θ_i with the normal. This choice of beam profile or cross-section greatly simplifies the analytic evaluation of the integrals in this and the next subsection. The profile of the beam is characterized by an effective width 2a that is large compared to the wavelength λ in the liquid. Therefore, the acoustic field has significant amplitude only for a distance a on either side of the beam axis. Consider the incident Gaussian beam at z = 0

$$\phi_f(x,0) = \frac{\Gamma_o \exp[-(x/a_o)^2 + ik_i x]}{\sqrt{\pi}\, a \cos\theta_i} , \qquad (18)$$

where Γ_o represents the amplitude of the potential in appropriate units; $k_i = k_f \sin\theta_i$ and $a_o = a\sec\theta_i$ is the half-width of the acoustic beam along the x-axis. Since the Fourier transform of (18) is

$$\Phi_f = \Gamma_o \frac{\exp[-(\xi - k_i)^2 (a_o/2)^2]}{\cos\theta_i} , \qquad (19)$$

the field of the reflected beam will be given by

$$\phi_f(x,z) = \frac{\Gamma_o}{2\pi} \int_{-\infty}^{\infty} R(\xi) \exp[-(\xi - k_i)^2 \left(\frac{a_o}{2}\right)^2] x$$

$$\exp[i\xi x - i\zeta_f z] \frac{d\xi}{\cos\theta_i} . \qquad (20)$$

Examination of Eq. (20) reveals that it cannot be inverted to give exact analytic results. However, the principal contribution to the integral comes from values of ξ lying in the vicinity of the incident wavenumber k_i. Accordingly, approximate values of $\phi_f(x,z)$ can be obtained by expanding ξ in a Taylor series about k_i. This entails approximations of $R(\xi)$ and $\zeta(\xi)$ for values of ξ close to k_i.

In adopting any form of approximation, care must be used. The straightforward approximation, such as the Taylor-series expansion, is adequate in ranges where $R(\xi)$ is well-behaved, specifically away from the surface-wave pole at $k_r + i\alpha$. If this fact is not taken into consideration, the results of this simple expansion for incident waves near or at the Rayleigh angle are inadequate to

explain the distortion of the reflected beam. By including the influence of the Rayleigh wave pole, Bertoni and Tamir [8] were able to explain these phenomena. In [8] it was also shown that Schoch's results are correct only for very wide beams. Before considering the influence of the Rayleigh wave pole on the reflected beam, we shall apply Schoch's approach to the present problem to obtain an expression for the beam displacement parameter Δ_s. By considering the case of total internal reflection ($\theta_i > \theta_c$), we may write the reflection coefficient in the form

$$R(\xi) = |R(\xi)|e^{iS(\xi)}, \tag{21}$$

where the amplitude $|R(\xi)|$ is very close to unity, and $S(\xi)$ is the phase of $R(\xi)$. Consistent with our previous approximation, the Taylor-series expansion about k_i is used for $S(\xi)$; this result is equivalent to a Fresnel expansion [8]. Then retaining the first term we obtain

$$R(\xi) \simeq R(k_i)\exp[i\{(\xi-k_i)S'(k_i)\}] \tag{22}$$

where $S'(k_i) = S(\xi)/\partial\xi$ evaluated at $\xi = k_i$. Similarly, by retaining three terms in the expansion of ζ_f we obtain

$$\zeta_f = \frac{k_f}{\cos\theta_i} - \xi\tan\theta_i - \frac{(\xi-k_i^2)^2}{2k_f\cos^3\theta_i} \tag{23}$$

Substitution from Eqs. (22) and (23) into Eq. (20) and comparing with Eq. (1a), it can be shown, for angles different from the Rayleigh angle, that the reflected beam profile at any location (x,z) is a modified Gaussian beam. Replacing x with x_r and a_o with a_r in accordance with the relations

$$x_r = x + z\tan\theta_i - S'(k_i) \tag{24}$$

$$a_r^2 = a_o^2 - \frac{2iz}{k_f\cos^3\theta_i} \tag{25}$$

we obtain what amounts to a shifting of the reflected beam along the x-axis by an amount

$$\Delta_s = - S'(k_i) , \tag{26}$$

along with the introduction of an effective complex beam width a_r.

It now remains to derive specific expressions for $S'(k_i)$. This can be done easily by differentiating Eq. (21) with respect to ξ. Noting that since $|R(\xi)|$ is approximately unity, we have

$$S'(k_i) = \frac{R'(k_i)}{iR(k_i)} . \tag{27}$$

Now, by rewriting $R(\xi)$ as

$$R = 1 - \frac{2F}{G + F} , \tag{28}$$

where

$$F = -(\rho_f\omega^2/\zeta_f)(\zeta_{1s}b_2 + \xi a_2) ,$$

$$G = a_1b_2 + a_2b_1 ,$$

we obtain

$$\Delta_s = -S'(k_i) = 2\left[\frac{F'G - G'F}{i(G + F)(G - F)}\right]_{\xi = k_i} \tag{29}$$

Substituting for F and G into Eq. (29), we obtain the lateral displacement of the reflected beam at or near the Rayleigh angle. Since F and G are functions of the frequency ω, Δ_s will also depend on ω in a manner that may be seen from Eq. (29). In the absence of the layer (h = 0), Eq. (53) yields the results that are reported by Schoch [2].

For the special case when the beam is incident at the Rayleigh angle, $\xi = k_r + i\alpha$, one finds that $G(k_r) \sim 0$ and Eq. (29) reduces to the form

$$\Delta_s = - S'(k_r) = - \frac{2iG'(k_r)}{F(k_r)} . \tag{30}$$

Employing the expressions for F and G in the above equation, we obtain, after some algebraic manipulation,

$$\Delta_s = - (\lambda\rho_s/\rho_f)(rs)^{1/2}(T_fD_1/T_1D_2), \tag{31}$$

where

$$s = (c_{2s}/c_r)^2 , \quad r = (c_{2s}/c_f)^2 , \quad q = (c_{2s}/c_{1s})^2$$

$$s_{1o} = [\rho_o/(\lambda_o+2\mu_o)]^{1/2} = 1/c_{1o},$$

$$s_{2o} = (\rho_o/\mu_o)^{1/2} = 1/c_{2o}$$

$$\bar{\mu}_o = \mu_o/\mu_s , \quad \bar{E}_o = (\lambda_o+2\mu_o)/\mu_s$$

$$P_{1o} = s^2 - s_{1o}^2 , \quad P_{2o} = s^2 - s_{2o}^2$$

$$T = (s-1)^{1/2} , \quad T_1 = (s-q)^{1/2} , \quad T_f = (r-s)^{1/2}$$

$$D_1 = 16s - 4s(T/T_1 + T_1/T) - 8TT_1 - 8$$

$$- Q[(2T^2 + P_{1o})\bar{E}_o/T + (2T_1^2 + P_{2o})\mu_o/T_1]$$

$$D_2 = 1 - Q\bar{E}_oP_{1o}(T - s/T_1) ,$$

and

$$Q = 2hk_{2s} = 2h\omega/c_{2s}$$

In the absence of the layer Eq. (31) reduces to

$$\Delta_s = \frac{2\lambda\rho_s}{\pi\rho_f}\left[\frac{r(r-s)}{s(s-1)}\right]^{\frac{1}{2}} x$$

$$\left[\frac{1 + 6s^2(1-q) - 2s(3-2q)}{s-q}\right] , \qquad (33)$$

which is identical with the results obtained by Schoch (see also [13]).

The dependence of Δ_s/λ on the dimensionless frequency Q for a specific set of elastic constants discussed later is shown in Fig. 2. In addition to the explicit appearance of Q in Eq. (31), c_r contains an implicit dependence on frequency and layer thickness, which also modifies the behavior of Δ_s/λ. The correct value of c_r as a function of Q is obtained from Eq. (16). At Q = 0, corresponding to long wavelength or small layer thickness, the value of Δ_s/λ from Fig. 2 is quite close to the substrate material, as verified in Eq. (33). As the layer thickness or the frequency increases, Δ_s/λ decreases, approaching the value predicted by Eq. (33) for the material properties of the layer. In fact, as expected, the model does not retain validity much beyond Q = 1, considering the approximation implicit in Eqs. (9) and (10). However, the results seem fairly insensitive to the assumption of constant displacement across the layer, although we have determined that the sensitivity can be strongly dependent on the specific combination of properties of the layer and substrate. In any case good agreement with experimental measurements is observed up to $Q \simeq 1.5$ ($2h/\lambda \simeq 0.25$), as we show in Section IV.

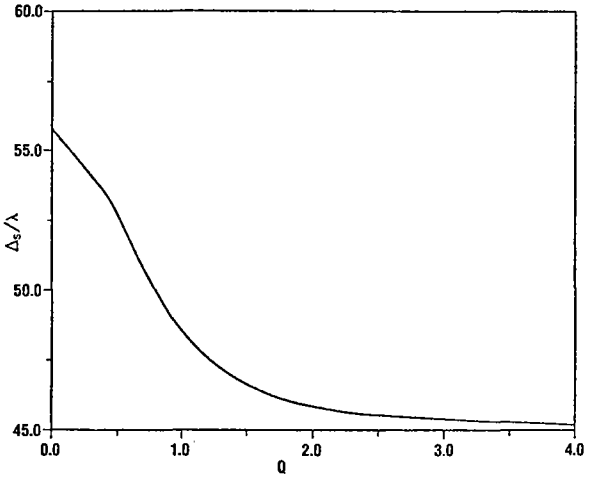

Figure 2 - Displacement parameter over wavelength plotted as a function of the dimensionless frequency-thickness product. Elastic constants are appropriate for a copper layer on stainless steel.

With the above results, the integral of Eq. (20) may now be evaluated. Following the procedure outlined in earlier work [8,14], the reflection coefficient in Eq. (14) is approximated by a truncated Laurent expansion about $\xi = k_r + i\alpha$, keeping only the first term. In this way we consider the influence of only the Rayleigh wave pole on the reflected field, and, correspondingly, the final result will be valid only when θ_i is at or near the Rayleigh angle. Since k_f is constant, the ξ dependence of ζ_f can be explicitly developed by a suitable expansion of terms in Eq. (12). After a change of variable, an application of the convolution theorem, and a contour integration around the upper half-plane, we obtain the final result for the wave potential of the reflected field at the Rayleigh angle

$$\phi_f' = \phi_{sp} + \phi_{lw} ,$$

where the subscripts "sp" and "lw" stand for specular and leaky wave, respectively. These two wave potential components of the reflected field are given explicitly from the above analysis by

$$\phi_{sp}(x,z) = -\frac{\Gamma_o \exp[-x^2/a_r^2]}{\sqrt{\pi}\, a_r \cos\theta_i} \exp[i(\xi x - \zeta_f z)] \qquad (34)$$

and

$$\phi_{lw}(x,z) = -2\phi_{sp}(1-\sqrt{\pi}\, a_r \exp[\gamma^2]\, \mathrm{erfc}(\gamma)/\Delta_s) , \qquad (35)$$

where

$$\gamma \equiv a_r/\Delta_s - x/a_r , \qquad (36)$$

erfc(Y) is the complimentary error function, and a_r is given by Eq. (25) neglecting $S''(k_i)$. It should be noted that apart from a generalization which includes the z dependence, Eqs. (34) and (35) are identical to Bertoni and Tamir's [8] result. This fact indicates that the modification of the reflected field due to the layer is contained entirely in the dispersive Rayleigh wavespeed c_r, the displacement parameter Δ_s, and the dimensionless frequency Q. The model presented here combines the new features that emerge in the layer case with previous results to yield an accurate, yet analytic, expression for the total reflected field.

EXPERIMENTAL PROCEDURE

Experiments in support of the theoretical development of the previous sections were performed to test dependences on important parameters of the model. We varied the layer thickness, ultrasonic frequency, incident angle, and transducer-interface separation distance in the course of many measurements on several samples. For rapid data acquisition and reduction an on-line computer was employed. The specimens used in these measurements are 302 stainless steel electroplated with high-purity copper. Both surfaces of the stainless steel plates (50 x 100 x 10 mm) are machine ground to assure parallelism, then abrasively polished to a mirror finish.

To permit as detailed a comparison with theory as possible, ultrasonic velocity measurements of a representative steel sample have been undertaken. We found the longitudinal wavespeed to be 5.69 $\pm$ .02 km/sec, while the transverse wavespeed is 3.13 $\pm$ .01 km/sec. These results are within 0.5% of the quoted values for 302 stainless steel [15].

For the copper layer we used literature values [16] of 4.76 km/sec and 2.2 km/sec, where the transverse wavespeed represents a 5% degradation of the value for bulk copper at room temperature. The densities are 8.93 g/cm^3 for copper and 7.9 g/cm^3 for stainless steel.

The transducers used in these experiments are either commercial wideband immersion-type transducers or specially designed "Gaussian beam" transducers. These latter are based on an earlier design [12] and consist of circular quartz plate resonators 2.5 cm in diameter with the water-side electrode completely covering one face, while the opposite face had a strip electrode either 6.4 mm or 3.6 mm in width. This configuration produced a beam whose amplitude distribution in the transducer midplane, perpendicular to the strip electrode accurately described a Gaussian profile, as we have verified in measurements at several frequencies. The Gaussian beam is essential since it corresponds to the incident beam profile assumed in the theoretical model of the previous section. For measurements to determine Rayleigh critical angles the wideband immersion transducers have proven more accurate. Data were acquired by fixing the position of the transmitting transducer with respect to the sample and scanning the receiving transducer across the reflected field, as indicated in Fig. 3. At each point in the discrete scan, the receiver comes to a complete halt, and the data point was read directly into the memory of an on-line computer. Then the receiver position is incremented automatically and the process repeated.

Comparing the measurements with the theoretical model of the previous section requires careful reduction of the data. We corrected the measurements on the basis of a calibration. Since the transducer voltage is proportional to the particle displacement, we obtained the following proportionality between wave potentials in Eqs. (34) and (35) and the transducer signal

$$A_{tr}(x,z) \sim |\phi_{sp} + \phi_{lw}| \ . \qquad (37)$$

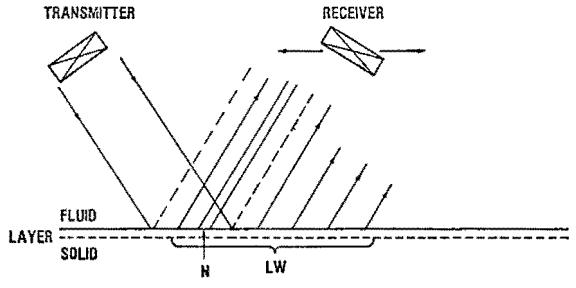

Figure 3 - Schematic of leaky wave experiment. Transmitter is fixed, while receiver scans along x-axis. Dashed lines in reflected field indicate specular reflection. Shaded regions contain most of the acoustic power. Null zone is denoted by N, and leaky wave reflected field by LW.

RESULTS AND DISCUSSION

Measurements of the Rayleigh wavespeed in three different samples as a function of Q ($= 2h\omega/c_{2s}$) are shown along with the theoretical prediction in Fig. 4. The quantity c_r is inferred by determining the Rayleigh angle with the following procedure. We adjusted transmitter and receiver in Fig. 3 to the same angle, then varied the receiver position and frequency until an absolute minimum in the null region was achieved. Changing angles, the procedure was repeated. From Eq. (31) the beam displacement parameter Δ_s decreases with increasing frequency until the null region become indistinct. Measurements at higher Q values may then be accomplished with a thicker layer. The three samples in Fig. 4 have progressively increasing layer thicknesses, spanning the region from $Q = 0$ to 3. A representative error bar indicates the uncertainty in the data points. Good overlap between the data sets lends confidence to the measurements, but the theoretical curve begins to deviate seriously from the data at about $Q = 1.5$. By $Q = 3$ this disparity has grown to 45% of the range of $c_r(Q)$. The size of this deviation has led us to try to fit other theoretical results in the literature. From this attempt we find that agreement between the approximate model presented here and more complicated exact results is strongly dependent on the specific material parameters of the substrate and layer. In particular as the ratio of substrate-to-layer wavespeeds increases, so does the observed agreement. As mentioned earlier, however, the nature of the assumptions suggests that some deviation beyond $Q = 1$ ($2h/\lambda \approx 0.2$) is not unexpected.

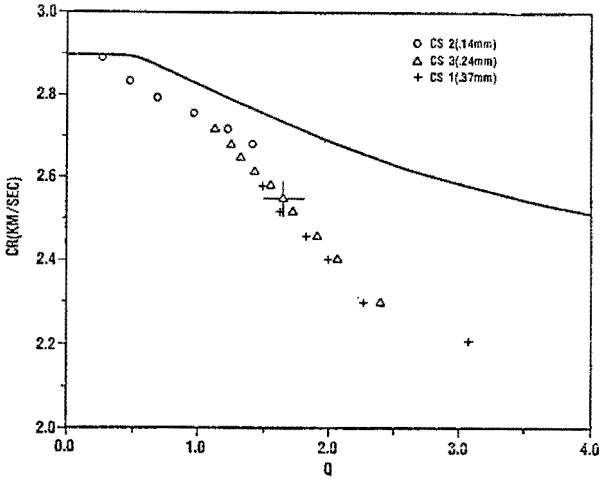

Figure 4 - Surface wave phase velocity plotted versus frequency-thickness product. Solid line is approximate theory, while experimental data points for three samples correspond to symbols indicated on graph. Typical error bars shown for a representative point.

The amplitude distribution curve for sample CS1 at a frequency of 1.5 MHz is shown as a function of receiver position in Fig. 5. These data are recorded by incrementing the x-coordinate of the receiver transducer with the transmitter in a fixed position. The individual points are the experimental data, while the solid curve is the theoretical result from Eqs. (34) - (37). In view of the disagreement between the theoretical value of $c_r(Q)$ and that inferred from Rayleigh angle

measurements, we have inserted the experimentally derived c_r into the expression for Δ_s from Eq. (31) used to derive the theory curve of Fig. 5. Because of signal averaging and system calibration, experimental uncertainty in the signal level is no larger than the plotting symbols in this and subsequent curves.

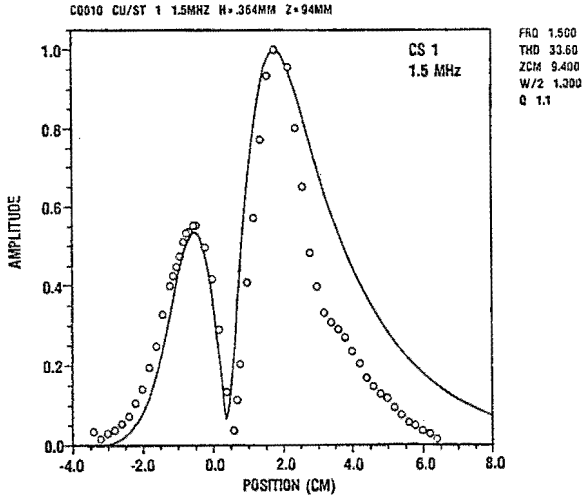

Figure 5 - Reflected acoustic field amplitude plotted versus receiver position for sample CS 1 at 1.5 MHz. Points are experimental data, and solid curve is theory from Eq. (62).

The features of the reflected field indicated schematically in Fig. 3 are apparent in a quantitative sense in Fig. 5. First, near x = -1.0 cm, a precursor peak appears, due to the coherent sum of ϕ_{sp} and ϕ_{lw} from Eqs. (34) and (35). At higher values of receiver position near x = 1.5 cm, a larger displaced reflection is observed, which arises mostly from the leaky-wave term. Between the two peaks is the null region where phase cancellation reduces the signal amplitude to near zero. Similar observations have been made in previous work [8,0]. From x = -3 to 3 cm agreement between the data of Fig. 5 and the theoretical prediction is relatively good. The precursor peak height and location of the null are fairly well predicted. Beyond x = 3.5 cm the experimental trailing field decreases more rapidly than predicted. This occurrence, noticed in several cases, is probably due to the finite y dimension of the Gaussian beam, which is only 20 mm long. When compared to an acoustic path length of 160 mm, the assumption of y-independent incident beam profile appears difficult to fulfill. We have determined the incident acoustic beam halfwidth from measurements at several frequencies with two transducers at varying separations. The wide transducer (6.4 mm) is used for generation, whereas the narrower one (3.6 mm) is the receiver. Inserting this estimate for a/2 into Eq. (25), we examine the theoretical fit, adjusting a/2 by no more than 10% to achieve the best effective width in light of the finite y extent of the transducer. Additional parameters used in the theory are summarized for this and subsequent curves in Table 1.

Figure 6 displays the amplitude distribution for sample CS2 for Q = .82. Here theory (solid curve) fits the data points somewhat better than the previous example, although there is still a tendency for the measured field to decrease slightly more rapidly than the model calculation. In addition, we have plotted for comparison the reflected field of the same beam at the same angle of incidence and frequency for a stainless steel sample with no layer present. Although the layer is rather thin ($2h/\lambda \simeq .15$), the effect on the reflected field is quite pronounced. The dashed curve, consisting of connected data points, indicates this field in Fig. 6. A small residual beam displacement remains since we are less than 2^o from the appropriate Rayleigh angle for the stainless steel surface (30.8^o). Far from all critical angles, the only contribution to the expression in Eq. (37) is ϕ_{sp}, and the undistorted beam would be centered on $x \doteq 0$.

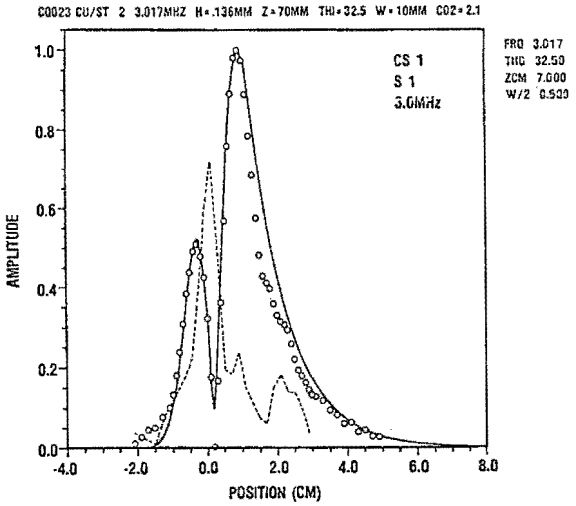

Figure 6 - Reflected acoustic field versus receiver position for sample CS 2 at 3 MHz. Experimental data are plotted discretely, solid curve is theory, and broken curve is experimental data for no-layer case.

As a first-order theory for acoustic reflection at fluid-solid interfaces loaded by a thin layer, the model we present here is quite adequate, particularly in the region $Q \geq 1$. However, several shortcomings should be pointed out. The calculation of c_r as a function of Q is prohibitively complicated. Expanding Eq. (16) and collecting coefficients of powers of the Rayleigh wavespeed reveals a characteristic equation which is 40^{th} order in c_r. Instead of proceeding in this manner, we have solved Eq. (16) implicitly for c_r by noting that the equation is only second order in Q. The difficulty with this method is that we know an exact complex solution for Eq. (16) at only one value of Q, namely, Q = 0. Developing a functional dependence of Q (c_r) for Q > 0 requires assumptions concerning the behavior of c_r in the complex plane. Fortunately, we are aided at this point by the fact that $\mathrm{Im}(c_r)/\mathrm{Re}(c_r) \ll 1$, implying that these assumptions do not seriously affect the results. A more general approach, however, would be needed to eliminate this problem and produce a result in better agreement with the data. Additional limitations are the assumption of the Gaussian beam profile and the intrinsic two-dimensionality of the analysis. The first of these could be circumvented by evaluating the reflected field numerically [10], but expanding the analysis to three dimensions would be a very significant complication.

Table 1 - Experimental Parameters

Figure	Sample	2h(mm)	Freq(Mhz)	Q	θ_i(deg)	z(mm)	a/2(mm)
5	CS 1	.37	1.5	1.1	33.6	94.	10.
6	CS 2	.14	3.0	.82	32.5	70.	5.
6	S 1	0.	3.0	0.	32.5	70.	5.

ACKNOWLEDGEMENTS

The authors are pleased to acknowledge helpful discussions with Dr. T. J. Moran. Capable technical assistance was given by D. L. Butler, R. D. Griswold, and K. D. Shimmin.

REFERENCES

1. F. Goos and H. Hañchen, Ann. Phys. (Leipzig) 1, 333 (1947).

2. A. Schoch, Acustica 2, 18 (1952).

3. A. Schoch, Ergeb. Exakten Naturwiss. 23, 127 (1953).

4. W. G. Neubauer, J. Appl. Phys. 44, 48 (1973).

5. W. G. Neubauer and L. R. Dragonette, J. Appl. Phys. 45, 618 (1974).

6. O. I. Diachok and W. G. Mayer, J. Acoust. Soc. Am. 47, 155 (1970).

7. W. G. Neubauer, Physical Acoustics, edited by W. P. Mason and R. N. Thurston (Academic Press, New York, 1973, Vol. X), 104-125.

8. H. L. Bertoni and T. Tamir, Appl. Phys. 2, 157 (1973).

9. M. A. Breazeale, L. Adler, and G. W. Scott, J. Appl. Phys. 48, 530 (1977).

10. L. E. Pitts, T. J. Plona, and W. G. Mayer, IEEE Trans. Sonics and Ultrason. SU-24, 101 (1977); T. D. K. Ngoc and W. G. Mayer, IEEE Trans. Sonics and Ultrason. SU-27, 229 (1980).

11. I. A. Viktorov, Rayleigh and Lamb Waves (Plenum Press, New York, 1967).

12. F. D. Martin and M. A. Breazeale, J. Am. Acoust. Soc. 49, 1668 (1971).

13. L. M. Brekhovskikh, Waves in Layered Media (Academic Press, New York, 1960) pp. 100-122.

14. T. Tamir and H. L. Bertoni, J. Opt. Soc. Am. 61, 1397 (1971).

15. H. E. Boyer, ed., Metals Handbook, Vol. II (American Society for Metals, Metals Park, Ohio, 1976).

16. G. W. C. Kaye and T. H. Laby, Tables of Physical and Chemical Constants (Longman, London, 1973).

17. Mini-manipulator available from Automation Industries, Inc.

William Pardee, Chairman (Rockwell Science Center): Are there any questions?

Unidentified Speaker: Have you included the effect of Lambda?

A.H. Nayfeh (Systems Research Laboratories): Yes, you remember I have included the effect of the layer in the boundary conditions.

Bill Reynolds (AERE, Harwell): I recall seeing some years ago some remarkable illustrations of this displacement on steel specimens which didn't, as far as I know, have a surface layer. Would your work suggest there was perhaps in this steel an atypical surface layer of material which was causing the effect?

A.H. Nayfeh: No. Surfaces without layers do exhibit the Schoch displacement. So what you're saying - Yes, we are saying that the shifting and modulation of the beam is due to the resonant coupling of energy from the beam in the fluid to the pseudo-Rayleigh wave in the surface. And this leads to a displacement and distortion of the reflected beam.

Mike Gardos (Hughes): To answer your question, the answer is yes. When you machine steel, you do have a damage layer on the surface as a matter of fact. You have a very significant subsurface damage layer, and these layers are themselves different from each other. So if you work with real specimens that you machine in a real world, you're going to see the difference in behavior. And if your method is sensitive to that, then you have something.

A.H. Nayfeh: But may I suggest that even smooth surfaces exhibit the displacement and distortion.

Laszlo Adler (Ohio State University): Let me make a point clear. The so-called Schoch displacement, which is a characteristic of the interface, includes the properties of both materials. The Schoch displacement is the parameter which describes the displacement of the reflected field.

A.H. Nayfeh: What you're suggesting could modulate the smooth surfaces. If our analysis is sensitive to this effect, then we might be able to isolate it.

William Pardee, Chairman: This is phenomena not precisely analogous to the effect of surface plasmons or surface plaritons in optics?

A.H. Nayfeh: We mentioned earlier it has been observed in optics.

William Pardee, Chairman: Are there any other questions: Thank you, Mr. Nayfeh.